Journal of Photochemistry and Photobiology A: Chemistry 208 (2009) 91–96

Contents lists available at ScienceDirect

Journal of Photochemistry and Photobiology A: Chemistry

journal homepage: www.elsevier.com/locate/jphotochem

The effect of porphyrin structure on binding to human serum albumin by fluorescence spectroscopy

Olga Rinco*, Janet Brenton, Alison Douglas, Amanda Maxwell, Michelle Henderson, Kirsten Indrelie, Jacob Wessels, Joan Widin

Department of Chemistry, Luther College, 700 College Dr., Decorah, IA 52101, USA

ARTICLE INFO

Article history:
Received 23 July 2009
Received in revised form 24 August 2009
Accepted 27 August 2009
Available online 2 September 2009

Keywords:
Porphyrins
Fluorescence
Singlet excited state
Host–guest interactions
PDT

ABSTRACT

The efficacy of porphyrin binding to human serum albumin (HSA) is critical to clinical use in photodynamic therapy (PDT). Several porphyrins were utilized to measure the effect of porphyrin structure on its binding to HSA. Two categories of porphyrins were utilized: porphyrins with a hydrophobic and hydrophilic side: Protoporphyrin IX (PPIX), Protoporphyrin IX dimethylester (PPIXDE), and Chlorin e_6 (Ce6) and porphyrins with hydrophilic substituents on both sides: Hematoporphyrin IX (Hme), Hematoporphyrin IX dimethylester (HmeDE), and Deuteroporphyrin IX dimethylester (DPIXEG). The following methods were used for the analysis: Stern–Volmer quenching, fluorescence lifetimes, anisotropy, fluorescence binding, and homogeneous studies. The results indicate that PPIX, PPIXDE, and Ce6 bind to HSA efficiently, evidence that porphyrins bind strongly to HSA if they have a hydrophobic and hydrophilic side. Hme is thought to bind to HSA but likely to a lesser degree than the aforementioned three porphyrins. HmeDE and DPIXEG seem not to bind to HSA probably due to the lack of hydrophobic substituents.

1. Introduction

Porphyrins are macrocycles composed of four pyrrole rings bridged by four sp^2 hybridized carbon atoms. The macrocycle is planar, fully conjugated and has a main conjugation pathway of 18 π electrons. These molecules are interesting photochemically and exhibit characteristics desirable for drug candidates in photodynamic therapy (PDT). These characteristics include: chemical purity, high quantum yield of singlet oxygen production, significant absorption at longer wavelengths, preferential tumor location, minimal dark toxicity, stability and the ability to dissolve in an injectable solvent system [1]. Porphyrins exhibit characteristic spectra with an intense Soret band (or B band) at 400 nm and usually four smaller Q-bands in the region between 500 and 600 nm. It has been shown that porphyrins currently used in PDT are capable of crossing the plasma membrane barrier of cells, in order to be incorporated in the cytoplasm, thus making them viable drug targets [2].

Protoporphyrin IX (PPIX) and Hemetaporphyrin (Hme) are clinically useful photosensitizers (PS) used in PDT of cancer and precancer legions [3]. It was in studying Hemetaporphyrin derivate in the 1970s that researchers realized that porphyrins could go beyond diagnostic agents, and in combination with light, had the capacity for tumor destruction [4–6]. PDT is gaining in popularity as a clinical treatment of cancer [1,7–10], and thus understanding relationships between potential PS and key biological hosts is of interest. Upon excitation with the proper wavelength of light, PS initiate photochemical reactions that lead to the formation of cytotoxic compounds (e.g. singlet oxygen). Previous studies have shown that at the time of PDT, PPIX is bound to either proteins and/or membranes [11]. Though some previous work has been done on the interaction of PPIX with proteins, most of this work has focused on plasma proteins [12–14]. One research group has focused on the binding of PPIX and PPIX photoproducts to small immunoglobulins [15,16], which are believed to be of importance for PDT [17]. The goal of the current study is to expand on these findings by examining the role that porphyrin structure (Scheme 1) plays on their ability to bind with human serum albumin (HSA). The series of porphyrins was chosen in order to study the effect of having hydrophilic branches on all sides of the porphyrin molecule (like Hme) vs. having a hydrophobic side and a hydrophilic side to the molecule (like PPIX).

HSA is a blood based protein that is used in drug distribution, and as such, it is important to know the affinity of any drug candidate for albumin. Early work has been carried out on the binding of Hme [18] as well as its derivatives [13] to HSA in addition to the studies mentioned for PPIX above, but no study has focused on the structural effect of the porphyrins in their ability to bind to HSA. It has been shown that porphyrins prefer to bind to sub domain IIA of HSA, which contains the lone tryptophan amino acid residue in the protein [18].

* Corresponding author. Tel.: +1 563 387 1684.
E-mail address: rincol01@luther.edu (O. Rinco).

1010-6030/$ – see front matter © 2009 Elsevier B.V. All rights reserved.
doi:10.1016/j.jphotochem.2009.08.009

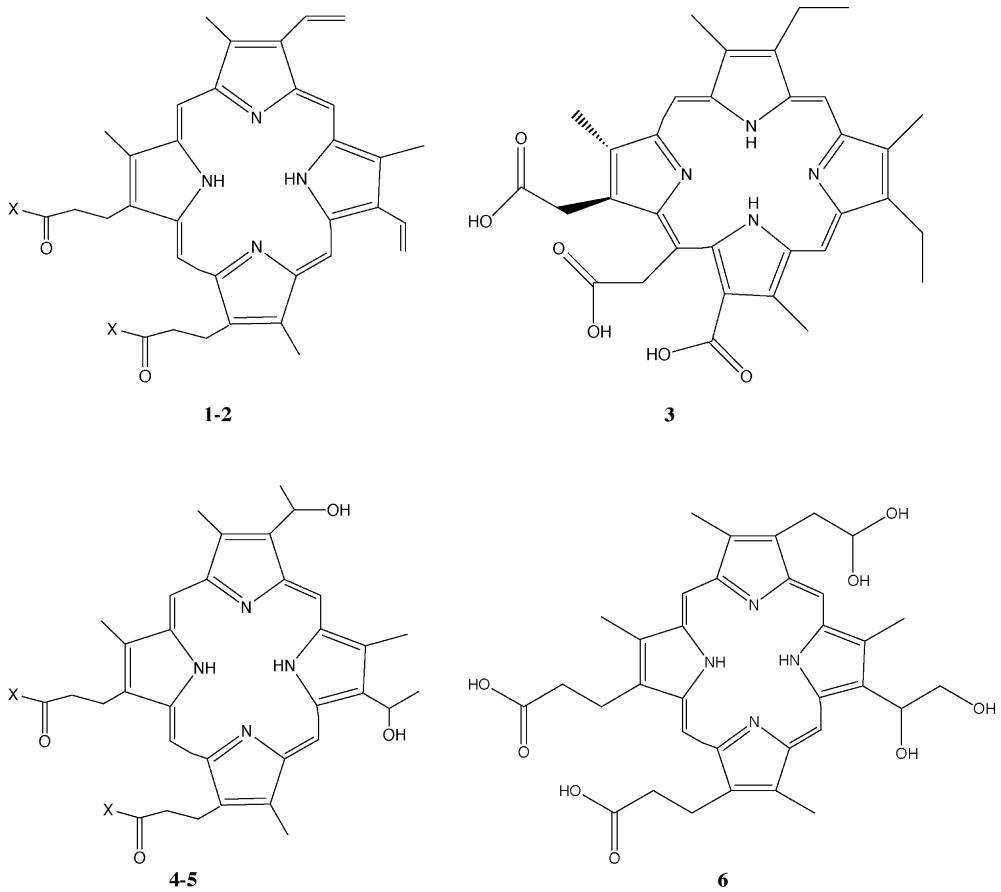

Scheme 1. Porphyrins under investigation: **1** Protoporphyrin IX (PPIX, X = OH), **2** Protoporphyrin IX dimethylester (PPIXDE, X = OCH_3), **3** Chlorine e6 (Ce6), **4** Hematoporphyrin IX (Hme, X = OH), **5** Hematoporphyrin IX dimethylester (HmeDE, X = OCH_3), **6** Deuteroporphyrin IX 2,4 bisethyleneglycol (DPIXEG).

Understanding the binding of porphyrins to HSA is vital to the success of these molecules being used in PDT, and the structural study is of interest in fundamental research on host–guest photochemistry. A systematic analysis of how altering the substitution pattern of the porphyrin will affect its ability to bind with HSA has not been reported. This study uses a mix of fluorescence spectral, quenching, anisotropy, binding and lifetime experiments to present the importance of a balance of hydrophobic and hydrophilic substitution patterns in order to allow porphyrins to bind to HSA.

2. Materials and methods

2.1. Materials

Sodium iodide (NaI; Spectrum, 99%), sodium phosphate (Na_2HPO_4; Flinn), potassium phosphate (KH_2PO_4; Fisher Scientific, 99.5%), albumin from human serum (Sigma, >96%), dimethyl sulfoxide (DMSO, C_2H_6OS; Acros), toluene ($C_6H_5CH_3$; Fisher Scientific, Class 1B), and methanol (CH_4O; Fisher Scientific, A935), were used as received. Millipore-Q filtered, deionized water was used for all samples.

The following porphyrins were all used as received from Frontier Scientific: Protoporphyrin IX (PPIX, $C_{34}H_{34}N_4O_4$, >97%), Deuteroporphyrin IX 2,4 bisethyleneglycol (DPIXEG, $C_{34}H_{38}N_4O_8$), Hematoporphyrin IX (Hme, $C_{34}H_{38}N_4O_6$), Protoporphyrin IX dimethylester (PPIXDE, $C_{36}H_{38}N_4O_4$), Deuteroporphyrin IX dimethylester (DPIXDE, $C_{32}H_{34}N_4O_4$ >97%), Chlorin e_6 (Ce6, $C_{34}H_{36}N_4O_6$; >95%), Hematoporphyrin IX dimethylester (HmeDE, $C_{36}H_{42}N_4O_6$; >97%)

2.2. Solution preparation

For most of the experiments outlined below, stock solutions of the various porphyrins were prepared. Small amounts of the stock solutions were injected into a 0.04 M phosphate buffer (pH 7.4) or 6 μM HSA. The stock solutions were prepared by dissolving a few crystals of the porphyrin in solvent (DMSO (PPIX, PPIXDE, Ce6), or methanol (Hme, HmeDE, DPIX)). The concentration of the porphyrins was between 5 and 10 μM. HSA solutions were prepared by dissolving the appropriate amount of the protein in the pH 7.4 phosphate buffer. To examine a physiologically relevant binding, all solutions containing HSA were heated to 37 °C for 0.5 h prior to any experiment. Fresh quencher solutions were prepared daily. A 2 M aqueous solution of NaI was used in the Stern–Volmer experiments outlined below.

2.3. Fluorescence studies

For all fluorescence experiments, ground state absorption spectra were recorded to assure the correct porphyrin concentration (based on absorption). An HP 8452A diode array spectrophotometer was used for all absorption measurements, and all samples displayed absorbances between 0.08 and 0.12 at the wavelength used for excitation in the fluorescence experiments. All samples were contained in 10 mm × 10 mm quartz cells made from Suprasil tubing.

Steady-state fluorescence measurements were carried out on a Jasco FP-6300 Spectrofluorometer or an Edinburgh FS900CDT T-Geometry Fluorometer (anisotropy measurements only). The excitation and emission slits were set so that the emission inten-

sity for each porphyrin was optimized. All samples were excited at their ground state absorption maxima (ca. 400 nm) and monitored for a ca. 300 nm range above the excitation wavelength. The fluorescence spectra were corrected for the baseline spectrum, which was a solution containing all components except the porphyrins. This procedure ensured that artifacts, such as Raman emission of the solvent, were subtracted from the fluorescence spectra.

Time resolved fluorescence measurements were carried out on an Edinburgh mini-τ compact lifetime system. The excitation source was a 405 nm picosecond pulsed diode light source (75 ps pulse duration, 130 mW power, and 100 kHz repetition rate). The emission was detected at the fluorescence emission maximum for each porphyrin. The interference filters were set so as to minimize the collection time, and a maximum of 10,000 counts was collected for the channel of maximum intensity. The instrument response function was measured using a millipore water sample. The data were fitted (using Edinburgh tail fit software) to a mono-exponential decay. In a few cases, a sum of two exponentials was needed, but each time this type of fit was needed to acquire reasonable fitting statistics it was noted that one of the two exponentials had a lifetime between 2 and 3 ns, and comprised less than 5% of the signal (usually closer to 2% of the decay). Thus, only one lifetime is reported for each porphyrin. The value of χ^2, the Durbin–Watson (DW) parameter, as well as a visual inspection of the residuals were used to determine how well the calculated decay fit the experimental data. Fits were considered acceptable when the χ^2 value was between 0.9 and 1.2, and the DW value was greater than 1.7.

2.3.1. Homogeneous studies

In the homogeneous experiments the porphyrins were dissolved directly in toluene or methanol, and the injection method described in Section 2.2 was used to dissolve the porphyrins in buffer and HSA solutions.

2.3.2. Stern–Volmer quenching studies

3 ml of sample (porphyrin in buffer or HSA) was placed in a 10 mm × 10 mm quartz cell. The 2 M NaI quencher was then added in increasing increments and a fluorescence spectrum was taken after each addition. A maximum of 300 μl of quencher was added to any given sample. A Stern–Volmer plot was generated for each study, with the fluorescence emission spectra area under the curve in the absence and presence of quencher (A_o/A), being plotted against the quencher concentration. All plots were linear and fit to the equation $A_o/A = 1 + K_{SV}[I^-]$, where K_{SV} is equal to the product of the quenching rate constant (k_q) and the lifetime of the porphyrin in the absence of quencher (τ_o).

2.3.3. Fluorescence anisotropy studies

A solution of porphyrin in buffer was created at concentrations appropriate to give absorbance readings of ca. 0.14 at the excitation wavelength for each individual porphyrin. 2.5 ml of this porphyrin/buffer solution was used in each sample and diluted with 1 ml of additional solution. The extra 1 ml of solution varied in HSA concentration and lead to final samples with HSA concentrations of 0–3 μM.

The samples were excited at the absorption λ_{max}, and the anisotropy was measured over a 4 nm window centered on the fluorescence emission λ_{max}. The rotational mobility (r) was obtained from the software, theory of anisotropy can be found in the literature [19]. A plot of the raw data (r vs. [HSA]) allowed r_F and r_B to be determined. r_F was the lower limit r value of the data and r_B was the r value at the high [HSA] end of the plot. Assuming no significant change in the porphyrin fluorescence intensity upon binding

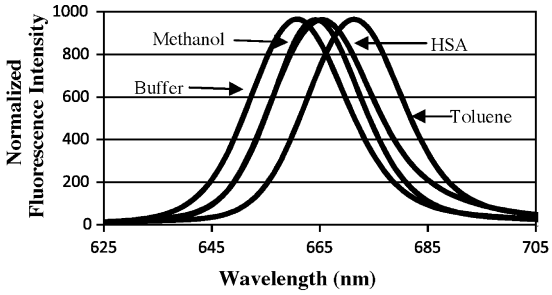

Fig. 1. Overlay plot of normalized fluorescence emission spectra of Ce6 in toluene, methanol, buffer and HSA.

($R = 1$), f_B was calculated for each [HSA], according to Eq. (1).

$$f_B = \frac{r - r_F}{R(r_B - r) + r - r_F} \quad (1)$$

Once f_B was determined for each solution, a double reciprocal plot of $1/f_B$ as a function of 1/[HSA] was created. A trend line was fit to the plot, and the data was analyzed according to Eq. (2):

$$\frac{1}{f_B} = \frac{1}{K_b}\frac{1}{[HSA]} + 1 \quad (2)$$

K_d, the dissociation constant, could then be calculated because it is the inverse of K_b. Therefore, the dissociation constant was the slope of the plot for each porphyrin.

2.3.4. Fluorescence binding studies

HSA shows a typical intrinsic fluorescence due to aromatic amino acids (tryptophan in particular) when excited at 280 nm. The addition of a porphyrin quenches the intrinsic fluorescence. This quenching can be used to retrieve the binding parameters by using the plot of $\log[(F_o - F)/(F - F_\infty)]$ against $\log[P]$, where F_o is the fluorescence of the protein in the absence of PPIX, F is the fluorescence of the protein at a concentration $[P]$ of PPIX and F_∞ is the fluorescence of the protein in solutions saturated with PPIX. The slope of the plot yields the number of binding sites, whereas the intercept $y = 0$ represents the dissociation constant [15,20].

3. Results

3.1. Homogeneous fluorescence studies

The purpose of performing homogeneous studies was to observe the fluorescence spectra of the porphyrins in solvents of varying polarities and the relative change in fluorescence with change in polarity. It was observed that all porphyrins studied displayed a blue shift in their fluorescence spectra with increasing solvent polarity as can be seen in Table 1. The experiments were carried out in toluene, methanol and buffer. Since blue shifts were observed it was reasonable to assume that if the porphyrin in the presence of HSA showed a red shift, compared to the buffer spectra (Fig. 1), it was possible that it was included within a binding site of HSA, which is less polar than the buffer solution surrounding the protein. This is in fact what was observed for all porphyrins except HmeDE and DPIXEG. PPIX, PPIXDE, Ce6 and Hme all had λ_{max} of fluorescence in HSA shifted to values between methanol and toluene and quite drastically different from the λ_{max} in buffer. A red shift in fluorescence emission spectra of porphyrins upon complexation with HSA is in agreement with previous reports for PPIX in HSA [14,15,20].

3.2. Stern–Volmer quenching studies

In most cases, the lifetime of a fluorescent probe molecule (like the porphyrins in this study) is much shorter than the lifetime of the

Table 1
Fluorescence emission maxima for the porphyrins in solvents of varying polarities to show whether or not red shifts in λ_{max} occur between buffer and HSA solutions.

Porphyrin	Solvent	λ_{max} (nm)	Porphyrin	Solvent	λ_{max} (nm)	Porphyrin	Solvent	λ_{max} (nm)
PPIX	Toluene	635	PPIXDE	Toluene	635	Ce6	Toluene	671
	MeOH	630		MeOH	631		MeOH	664
	Buffer	621		Buffer	623		Buffer	661
	HSA	634		HSA	633		HSA	665
Hme	Toluene	628	HmeDE	Toluene	626	DPIXEG	Toluene	625
	MeOH	625		MeOH	622		MeOH	622
	Buffer	614		Buffer	613		Buffer	613
	HSA	625		HSA	615		HSA	614

dynamic processes occurring between the probe and the host (HSA) [21]. As such, the probe molecules are able to report on the environment in which the probe is located, and point to a difference in binding affinity for different porphyrins to HSA. Fluorescence quenching experiments were used in this study to give an indication of the porphyrin's incorporation within the HSA binding sites, as the quenching rate constant (k_q, Table 2) is a measure of the accessibility of the quencher to the porphyrin within HSA.

Deactivation of the singlet excited state of the various porphyrins was studied using sodium iodide (NaI) as a quencher [22]. Since the quencher used is in this study is an aqueous quencher, it is expected that the quenching efficiency will be greater if the porphyrin is not included in the binding site(s) of HSA than if it is included in a binding region. Upon addition of NaI, the fluorescence emission intensity of all the porphyrins was observed to decrease. The data from these spectra were analyzed in order to extract the Stern–Volmer constant (K_{SV}) for the porphyrins in the presence and absence of HSA. Following the equation in Section 2.3.2, K_{SV} was obtained from the slope of the plot (Fig. 2).

The K_{SV} is a product of the quenching rate constant (k_q) and the intrinsic lifetime (τ_o) of the porphyrin. Thus to truly discuss the k_q, fluorescence lifetimes of the porphyrins in the presence and absence of HSA were determined (Table 2). Once all the lifetimes were determined the quenching rate constant was calculated by dividing the K_{SV} by the τ_o of the porphyrins (Table 2). From Table 2, it can be stated that the k_q for DPIXEG did not change in the presence of HSA. Also, it appears that the k_q for HmeDE increases in the presence of HSA, though it is believed that there simply is no change in the quenching between buffer and HSA, and the numbers are within experimental error. For all of the other porphyrins (PPIX, PPIXDE, Ce6 and Hme) a distinct decrease in the value of k_q upon the introduction of HSA was observed. The decrease in k_q is attributed to the porphyrins being in a less accessible location for the aqueous quencher (i.e. within a binding region of HSA).

A brief study to confirm the mechanism of quenching was undertaken. In place of steady-state fluorescence quenching (plotting A_o/A), two time resolved quenching experiments (plotting τ_o/τ) were performed. The experiments were performed on PPIX (thought to be binding to HSA) and DPIXEG (thought to be excluded from binding in HSA). In both cases, the K_{SV} recovered for the plot agreed with the values presented in Table 2 and thus, dynamic quenching does appear to be the mechanism in this case, and interaction of the quencher and porphyrin in solution before excitation is not likely.

Table 2
Fluorescence parameters: Stern–Volmer constants (K_{SV}) recovered from aqueous quenching with NaI, intrinsic lifetimes (τ_o), and quenching rate constants (k_q) in the absence and presence of HSA. Number in parenthesis represents number of times experiment was performed, and errors are average deviations (2 trials) and standard deviations (more than 2 trials).

Porphyrin	Solvent	K_{SV} (M^{-1})	τ_o (ns)	k_q (M^{-1} s^{-1})
PPIX	Buffer	30 ± 2 (3)	17.0 ± 0.5 (2)	1.8 ± 0.1
	HSA	13 ± 4 (3)	14 ± 2 (3)	0.9 ± 0.3
PPIXDE	Buffer	13 ± 2 (3)	17 ± 3 (3)	0.7 ± 0.2
	HSA	4.6 ± 0.5 (3)	15.5 ± 0.1 (2)	0.30 ± 0.03
Ce6	Buffer	22 ± 9 (4)	4.3 ± 0.3 (3)	5 ± 2
	HSA	20 ± 3 (4)	5.3 ± 0.3 (2)	3.8 ± 0.6
Hme	Buffer	15 ± 2 (3)	16.75 ± 0.04 (3)	0.9 ± 0.1
	HSA	9.9 ± 0.6 (3)	17.22 ± 0.06 (2)	0.57 ± 0.03
HmeDE	Buffer	22 ± 3 (3)	16.8 ± 0.2 (3)	1.3 ± 0.2
	HSA	37 ± 16 (3)	17.3 ± 0.3 (2)	2.1 ± 0.9
DPIXEG	Buffer	12 ± 2 (3)	16.6 ± 0.1 (2)	0.7 ± 0.1
	HSA	13.3 ± 0.2 (3)	17.0 ± 0.3 (2)	0.78 ± 0.02

3.3. Fluorescence anisotropy studies

The purpose of performing anisotropy studies was to determine the rotational mobility (r) and from that extract the binding constant (K_b) from which the dissociation constant (K_d) for each porphyrin was calculated. Fluorescence anisotropy is an experimental measurement of fluorescence depolarization. When a fluorescent molecule is excited by polarized light, the emission given off is also polarized. The main cause of fluorescence depolarization is rotational diffusion of the fluorophore during the time period in which it is in its excited state. Fluorescence polarization measurements can be used to determine the rotational mobility of the fluorophore [19]. If the porphyrin (in this case) is not bound tightly, it is expected that it will be more freely rotating, thus the rotational diffusion will be large. If the porphyrin is more restricted (within the binding regions of HSA), the rotational diffusion will be decreased with increasing HSA concentration, and a change in the rotational mobility will be observed.

The experiments were carried out and fitted according to Eqs. (1) and (2), and the data is presented in Table 3. PPIXDE's fluorescence signal was too weak to perform anisotropy experiments to any degree of satisfaction, thus these results cannot be analyzed. HmeDE and DPIXEG showed no change in rotational mobility with increasing HSA concentration, and thus it is believed that the rota-

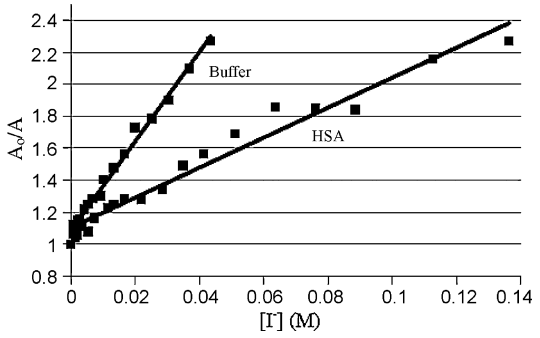

Fig. 2. Stern–Volmer quenching plot of PPIX in the presence of buffer and HSA. Plot of the fluorescence intensity in the absence and presence of quencher against the quencher concentration.

Table 3
Porphyrin binding constants to HSA recovered from fluorescence anisotropy experiments. Number in parenthesis represents number of times experiment was performed, and errors are standard deviations.

Porphyrin	K_d (μM)
PPIX	0.8 ± 0.4 (6)
PPIXDE	N/A[a]
Ce6	0.93 ± 0.51 (5)
Hme	1.30 ± 0.06 (3)
HmeDE	N/A[b]
DPIXEG	N/A[b]

[a] Fluorescence signal too weak to obtain data.
[b] No change in rotational mobility observed.

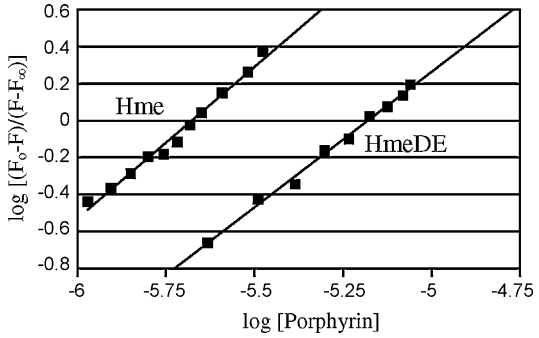

Fig. 3. Binding of Hme and HmeDE to HSA measured from the emission of the proteins. Plots are obtained by following the changes of protein intrinsic fluorescence (excitation at 280 nm).

tional mobility of these porphyrins was not affected by the presence of the protein. PPIX, Ce6 and Hme all had measurable differences in rotational mobility, thus appearing to be interacting with the HSA. Dissociation constants (K_d) were also calculated for the three porphyrins which displayed anisotropic results. No great difference was observed in the dissociation constants within error, however the values for PPIX and Ce6 were always slightly lower than those for Hme. Slower dissociation would suggest stronger binding to the HSA binding site(s).

3.4. Fluorescence binding studies

The addition of porphyrin to solutions containing HSA caused the quenching of the intrinsic protein fluorescence (due to amino acid residues). Like the anisotropy studies above, protein fluorescence quenching can also be used to retrieve porphyrin–HSA binding parameters (Fig. 3) [20]. The parameters obtained from plots like Fig. 3 (K_d and number of binding sites) are consistent with the presence of two binding sites (Table 4) and dissociation constants similar to those published previously (for PPIX, 4.8 ± 5 μM) [15]. Dissociation constants are difficult to reproduce with great accuracy and many previous published numbers have large errors associated with the values, thus it is a trend in the data that was being sought as well as support of the other information presented in this paper. The value of the dissociation constants in the fluorescence binding studies differ from those recovered from the anisotropy data, but the trend in data is similar. As can be seen from Table 4, the K_d for PPIX, PPIXDE and Ce6 as a group are lower than those of HmeDE, and DPIXEG. Hme appears to belong more with the first group than the second. Again, the lower the dissociation constant the more tightly the porphyrin is believed to be bound to the HSA.

Table 4
Binding parameters for porphyrins binding to HSA recovered from fluorescence binding studies. Number in parenthesis represents number of times experiment was performed, and errors are standard deviations.

Porphyrin	K_d (μM)	Number of binding sites
PPIX	2.6 ± 0.9 (4)	1.62 ± 0.07 (4)
PPIXDE	3.9 ± 0.3 (3)	1.7 ± 0.2 (3)
Ce6	2.7 ± 0.5 (3)	1.84 ± 0.09 (3)
Hme	3.1 ± 0.4 (3)	1.7 ± 0.3 (3)
HmeDE	7 ± 3 (4)	1.4 ± 0.2 (4)
DPIXEG	4.4 ± 1.7 (4)	1.8 ± 0.4 (4)

4. Discussion

The collective data presented in Section 3 suggests that binding of the porphyrins to HSA is stronger when the molecule contains a hydrophobic side and a hydrophilic side (PPIX, PPIXDE and Ce6) than when the molecule is hydrophilic on all sides (Hme, HmeDE and DPIXEG). Experiments on porphyrins with all hydrophobic sides (i.e. octaethylporphine) were inconclusive due to solubility issues and are thus not reported in this current publication. The data suggests that a hydrophobic side of the molecule is necessary to drive the porphyrin into the protein binding regions, and the hydrophilic side helps with its ability to be soluble in the solution.

PPIX, PPIXDE and Ce6 show signs of being included in the HSA binding site in all the experiments. In the homogeneous studies, the fluorescence emission spectra in HSA was red shifted compared to that in buffer. In the fluorescence quenching studies a decrease was observed in the k_q for all three porphyrins in HSA compared to the k_q value in buffer. PPIX's value for k_q was decrease by 50%, PPIXDE's value was decreased by 57% and the k_q for Ce6 was decreased by 24%. In the fluorescence anisotropy, PPIXDE could not be evaluated due to a weak fluorescence polarization signal. PPIX and Ce6 exhibited increasing restriction to rotational mobility with increasing HSA concentration. Dissociation constants very close to 1 μM were recovered from the anisotropy study for both porphyrins. Thus, anisotropy suggests that these porphyrins are well bound in an HSA binding site which limits mobility. Finally, in the protein fluorescence binding studies, dissociation constants in the 2–3 μM range were recovered for these three porphyrins, which were lower than those recovered for HmeDE and DPIXEG. Lower dissociation suggests that these porphyrins are more tightly bound to the HSA binding sites.

The Hme data suggests binding to HSA, though potentially to a lesser extent than the three porphyrins discussed above. The homogeneous data shows a red shifted fluorescence emission spectra in HSA compared to buffer. The quenching data showed a 37% decrease in k_q. In the fluorescence anisotropy study, a dissociation constant just above 1 μM was recovered and this value increased to 3 μM in the fluorescence binding studies. It was noted that in any comparison of Hme to PPIX or PPIXDE on a given day, the Hme K_d was always larger than the other porphyrin's recovered K_d. There is no doubt that Hme binds to HSA, but the extent of the binding is unclear.

The two other hydrophilic porphyrins (HmeDE and DPIXEG) do not appear to bind with HSA. The initial homogeneous studies show little or no shift in the fluorescence emission maximum between buffer and HSA solutions. In the quenching experiments again, there is no change in the quenching efficiency of the porphyrins in the presence or absence of HSA. As noted previously for HmeDE, it actually appears that the quenching rate constant increases in HSA, but it is believed that the quenching efficiency is truly the same as in buffer. Furthermore, though the quenching experiments in HSA were all linear, the fits were not as good (based on R^2 values) as those in buffer. This is expected as the binding of porphyrins with HSA leads to a more complicated system. The HSA quenching data for the other four porphyrins had R^2 values lower (closer to 0.90) than the experiments in buffer (closer to 0.99). For

HmeDE and DPIXEG however, the R^2 values were just as good as those observed in buffer, again suggesting that these porphyrins are residing in the buffer bulk as opposed to bound within HSA. The anisotropic experiments were perhaps most convincing as no change in rotational mobility was observed over the entire range of HSA concentrations. The confusing data comes from the quenching of the intrinsic fluorescence of the protein where the dissociation constants are higher than the other porphyrins, but the number of binding sites recovered is similar to the porphyrins which appear to bind to HSA. This lead to the belief that this study is perhaps the least impactful of all attempted in the current work. The overall trend in the data however is reasonably convincing. All of this leads to the suggestion that porphyrin structures that contain some hydrophobic moieties will increase the potential for the porphyrin to bind with HSA.

One possibility to explain the slight differences in binding between the PPIX series of porphyrins and Hme would be binding to different sites within the HSA molecule. To test whether or not either Hme or PPIX appeared to be binding to two different sites, a study looking at fluorescence lifetimes at short and long timescales and at varying concentrations of HSA was carried out. The study looked at HSA concentrations between 0 and 6 μM and both short and long time scales were observed. All of the fits gave rise to the same lifetimes (reported in Table 2). Lifetimes were also checked at various fluorescence emission wavelengths (sort and long) and all of the fits gave rise to the same lifetimes reported above. Fluorescence lifetimes of photosensitizers are often sensitive to their binding location in biological systems, thus it is most likely that the porphyrins are binding to one site preferentially in the protein. It is possible that Hme is binding to a different site than PPIX.

5. Conclusions

This study confirmed that the binding of porphyrins to HSA is increased if the structure of the porphyrin contains hydrophobic branches as well as hydrophilic branches off of the tetrapyrrole conjugated ring structure. PPIX, PPIXDE and Ce6 appear to bind most strongly with HSA. Hme, contains hydrophilic subsitituents on all four branches and does appear to bind with HSA, but HmeDE and DPIXEG, which also contain four hydrophilic branches do not appear to be including in HSA binding sites. Though numerous experiments supported this result, the fluorescence anisotropy study is the most definitive, showing a clear lack of binding for HmeDE and DPIXEG.

Acknowledgments

The authors thank the Monticello College Foundation and the Iowa College Foundation – R.J. McElroy Trust for partial financial support of this research, as well as Luther College's faculty/student collaborative research grants for allowing numerous students the opportunity to work on this project. The authors also acknowledge the contribution of other group members who were present during this work: Nicholas Gibbons, Alison Rapacz Knutson, Jennifer Miller Meyer and Jay Dicke.

References

[1] R.K. Pandey, G. Zheng, Porphyrins as photosensitizers in photodynamic therapy, in: K.M. Kadish, K.M. Smith, R. Guilard (Eds.), The Porphyrin Handbook, New York, 2000, pp. 157–230.
[2] A.S. Chakraborti, Interaction of porphyrins with heme proteins—a brief review, Mol. Cell. Biochem. 253 (2003) 49–54.
[3] B.W. Henderson, T.J. Dougherty, How does photodynamic therapy work? Photochem. Photobiol. 55 (1992) 145–157.
[4] I. Diamond, S.G. Granelli, A.F. McDonagh, C.B. Wilson, R. Jaenicke, Photodynamic therapy of malignant tumors, Lancet 2 (1972) 1175–1177.
[5] J.F. Kelly, M.E. Snell, Hematoporphyrin derivative: a possible aid in the diagnosis and therapy of carcinoma of the bladder, J. Urol. 115 (1976) 150–151.
[6] T.J. Dougherty, G.B. Grindey, R. Fiel, K.R. Weishaupt, D.G. Boyle, Photoradiation therapy II. Cure of animal tumors with hematoporphyrin and light, J. Natl. Cancer Inst. 55 (1975) 115–121.
[7] Z. Huang, Photodynamic therapy in China: over 25 years of unique clinical experiences: part one-history and domestic photosensitizers, Photodiagn. Photodyn. Ther. 3 (2006) 3–10.
[8] D.Y. Xu, Research and development of photodynamic therapy photosensitizers in China, Photodiagn. Photodyn. Ther. 4 (2007) 13–25.
[9] J.N. Silva, P. Filipe, P. Morliere, J.C. Maziere, J.P. Freitas, J.L. Cirne de Castro, R. Santus, Photodynamic therapies: principles and present medicinal applications, Bio-Med. Mater. Eng. 16 (2006) S147–S154.
[10] J. Moan, K. Berg, Photochemotherapy of cancer: experimental research, Photochem. Photobiol. 55 (1992) 931–948.
[11] J. Moan, G. Streckyte, S. Bagdonas, O. Bech, K. Berg, Photobleaching of protoporphyrin IX in cells incubated with 5-aminolevulinic acid, Int. J. Cancer 70 (1997) 90–97.
[12] S. Cohen, R. Margalit, Binding of porphyrin to human serum albumin, Biochem. J. 270 (1990) 325–330.
[13] L.I. Grossweiner, G.C. Goyal, Binding of hematoporphyrin derivative to human serum albumin, Photochem. Photobiol. 40 (1984) 1–4.
[14] M. Beltramini, P.A. Firey, F. Ricchelli, M.A.J. Rodgers, G. Jori, Steady-State and Time-Resolved Spectroscopic Studies on the Hematoporphyrin-Lipoprotein Complex, Biochemistry 26 (1987) 6852–6858.
[15] L. Brancaleon, H. Moseley, Effects of photoproducts on the binding properties of protoporphyrin IX to proteins, Biophys. Chem. 96 (2002) 77–87.
[16] L. Brancaleon, S.w. Magennis, I.D.W. Samuel, E. Namdas, A. Lesar, H. Mosely, Characterization of the photoproducts of protoporphyrin IX bound to human serum albumin and immunoglobulin G, Biophys. Chem. 109 (2004) 351–360.
[17] C.J. Gomer, Preclinical examination of first and second generation photosensitizers used in photodynamic therapy, Photochem. Photobiol. 54 (1991) 1093–1107.
[18] E. Reddi, F. Ricchelli, G. Jori, Interaction of human serum albumin with hematoporphyrin and its Zn^{2+} and Fe^{3+} derivatives, Int. J. Peptide Protein Res. 18 (1981) 208–402.
[19] J.R. Lakowicz, Principles of Fluorescence Spectroscopy, second ed., Kluwer Academic/Plenum Publishers, New York, 1999.
[20] B.M. Aveline, T. Hasan, R.W. Redmond, The effects of aggregation, protein binding and cellular incorporation on the photophysical properties of benzoporphyrin derivative monoacid ring A (BPDMA), J. Photochem. Photobiol. B. 30 (1995) 161–169.
[21] M.H. Kleinman, C. Bohne, Use of photophysical probes to study dynamic processes in supramolecular structures, in: V. Ramamurthy, K.S. Schanze (Eds.), Organic Photochemistry: Molecular and Supramolecular Photochemistry, vol. 1, New York, 1997, pp. 390–465.
[22] S.L. Murov, I. Carmichael, G.L. Hug, Handbook of Photochemistry, second ed., Marcel Dekker, Inc., New York, 1993.